JOURNAL OF MATERIALS SCIENCE **34** (1999) 3057 – 3061

Effect of Na-diffusion on the electrical properties of $SrTiO_3$

SEONG-HO KIM, JAE-DONG BYUN
Department of Materials Science and Engineering, Korea University, 136-701, Seoul, Korea
WON-PARK
Department of Chemical Engineering, University of Toronto, ON, Canada
YOONHO KIM
Division of Ceramics, Korea Institute of Science and Technology, P.O. Box 131, Seoul, Korea
E-mail: gojira@kist.re.kr

Grain boundary characteristics of Na-diffused $SrTiO_3$ were investigated. It was observed that Na ions are segregated in grain boundaries by secondary ion mass spectroscopy analysis. Using *I-V* characteristics and *C-V* measurement, the non-linearity coefficient and the potential barrier height were found to be 15.6, 0.82 eV, respectively. The *I-V* characteristics, complex plane analysis, and dc voltage step technique were performed to study the electrical properties of a single grain boundary. From the results of complex plane analysis, the deep electronic level was varied from 0.10 to 0.31 eV, which can be explained by the substitution of Na ions for Sr ions. © *1999 Kluwer Academic Publishers*

1. Introduction

$SrTiO_3$ is one of the most important electroceramic materials [1, 2]. When doped with proper dopants and fired in reducing atmosphere, it is known to show semiconductive characteristics [3–5]. It is also used as a material for producing a grain boundary barrier layer capacitor (GBBLC) which has insulating grain boundaries and semiconductive grains [6–9]. More recently, a new-type of $SrTiO_3$ has been reported, which has not only a high dielectric constant, but also non-ohmic electrical characteristics [10, 11]. Since the dielectric constant of $SrTiO_3$ is 100–1000 times larger than that of ZnO, a $SrTiO_3$ varistor shows a large surge capability and a sharp pulse response [12]. Therefore, it can be used as a capacitor-varistor as well [13, 14].

Generally, the fabrication of $SrTiO_3$-based varistor is done by a two-step firing method, in which a specimen is sintered with dopant in reducing atmosphere to make semiconductive grains and then alkaline ions are diffused in postsintering heat treatment [10, 11]. By Na-diffusion along grain boundaries, a potential barrier such as double-Schottky barrier is formed between grains and grain boundaries. Fujimoto *et al.* has reported that the source of potential barrier height on a grain boundary layer is substitution of Sr sites for Na ions [10]. Since Na is an acceptor that has a considerable strain energy driving force for segregation due to the misfit in ionic radii, the segregation of Na ions produce the potential barrier height. Zou and Meng observed the diffusion and distribution of Na ions by HRTEM and STEM-EDX [15]. However, there have not been many investigations that covered change in the electrical properties of grains and grain boundaries layer due to Na-diffusion.

In this study, Secondary ion mass spectroscopy (SIMS) was employed to ensure the profile of Na-diffusion along the grain boundary and an investigation on the changed electrical properties of $SrTiO_3$ with the diffusion of Na was carried out using a micro-electrode method.

2. Experimental

Ceramic specimens were prepared by a conventional mixed-oxide route, starting from 1.00 mol of $SrCO_3$, 1.01 mol of TiO_2, and 0.006 mol of Nb_2O_5. Powder mixtures were wet-milled for 12 h and then completely dried at 150 °C. After drying, the powders were calcined at 1200 °C for 2 h. Each specimen was pressed under 100 MPa into a disk-shape of 10 mm in diameter and 1.5 mm in thickness and fired at 1570 °C for 8 h in reducing atmosphere (90% N_2 + 10% H_2). Na_2O pastes were painted on the top of specimen and annealed at 1000 °C for 1 h in air. In order to compare the electrical property of air-diffused (without the diffusion of Na) specimen, the specimens were annealed at 1000 °C for 1 h in air. The specimens annealed with Na and without Na were termed as $N1$ and $N2$, respectively. After polished carefully and chemically etched, the diffusion profile of Na in the specimen was obtained by TOF-SIMS (7200, PHI, USA). The dielectric properties of specimens were measured with Ag-electrode using an impedance/gain-phase analyzer (4724A, Hewlett-Packard, USA). *C-V* measurements of the bulk specimen were carried out by an impedance/gain-phase analyzer (4194A, Hewlett-Packard, USA). *I-V* characteristics were employed by a high voltage source measurement unit (237, Keithly, USA). For the

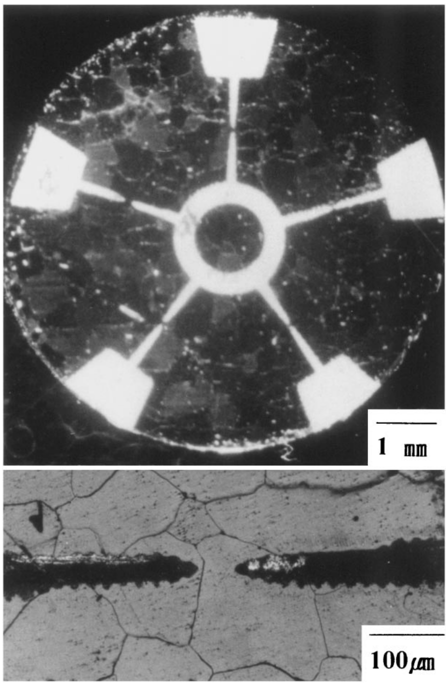

Figure 1 Optical micrographs of polished surface with micro-electrodes.

measurements of I-V characteristics, complex plane analysis, and dc voltage step technique of a single grain boundaries, the specimens were polished and micro-electrodes were formed with Pt pastes at polished surfaces of sintered specimens as illustrated in Fig. 1.

3. Results

3.1. SIMS analysis

A grain boundary is known as more dominant diffusion path of solute than a grain [16]. In this study, SIMS analysis was employed to ensure that Na ions segregate in grain boundaries and was performed in 100×100 μm region (Fig. 2). In order to avoid any contamination on the surface, sputtering was carried out in chamber for 30 min. The map of SIMS analysis indicated that Sr and Ti uniformly existed throughout most of specimen and Na ions segregated in grain boundary layers. The map of Sr and Ti show the enrichment of Ti in near grain boundaries. The stoichiometry of Sr and Ti in grain boundary layers was not confirmed, however, because of the limitation of SIMS analysis.

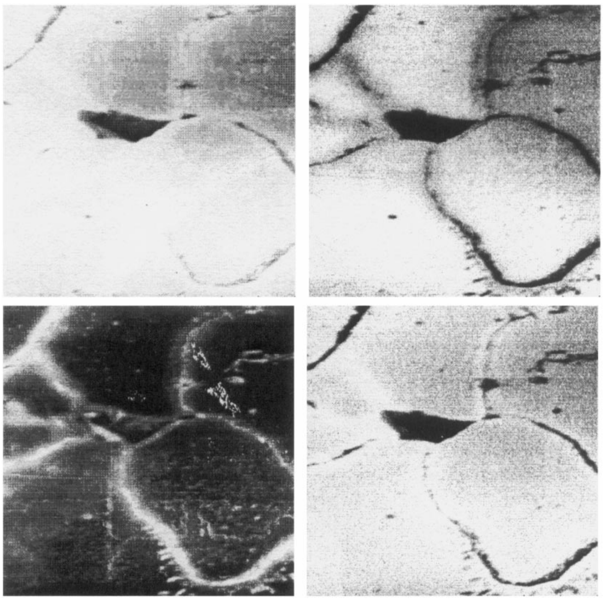

Figure 2 SIMS micrographs of a representive region of the Na-diffused $SrTiO_3$. Clockwise from left corner: total, Sr, Ti, and Na ion maps. Images are taken from 100×100 μm^2 area.

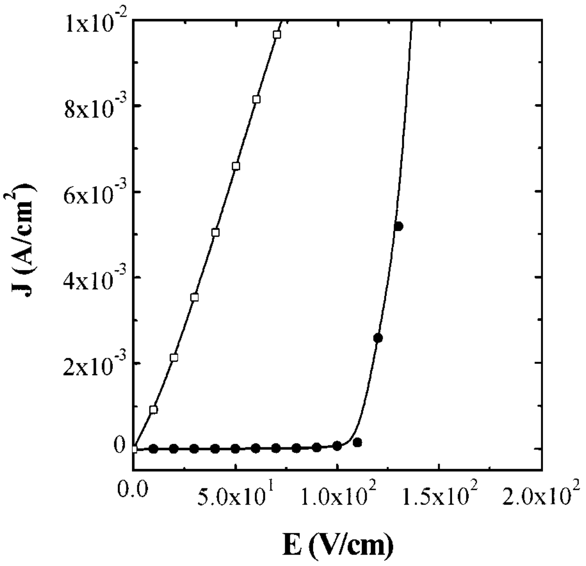

Figure 3 I-V characteristics of bulk specimen: □, without Na-diffusion; ●, with Na-diffusion.

3.2. *I*-*V* characteristics

Dielectric constants and non-linearity coefficients of specimens were listed in Table I. Fig. 3 shows the I-V characteristics of bulk specimens, $N1$ and $N2$. When Na ions were diffused in the sintered specimen, the non-linearity coefficient was reached to 15.6, whereas that of specimen annealed in air was a relatively low-value, about 5. In order to observe the I-V characteristics of a single grain boundary, a micro-electrode method was employed in this study. From the obtained I-V curves as shown in Fig. 4, the non-ohmic behavior in grain boundary layer was substantially observed. The I-V curves of Na-diffused $SrTiO_3$ at various temperatures were shown in Fig. 5. The I-V characteristics revealed that log I is proportional to $V^{1/2}$ below the breakdown voltage, similar to behaviors of ZnO varistors [17]. Therefore, it can be concluded that the conduction mechanism at below breakdown voltage depends on the thermoionic conduction-emission process.

3.3. *C*-*V* measurement

The potential barrier height and the donor concentration of specimen were determined by measurements of C-V relationship [18, 19]. The donor concentration (N_d) in bulk and the potential barrier height (ψ) at grain boundaries can be determined by following Equation 1:

$$\left(\frac{1}{C} - \frac{1}{2C_0}\right)^2 = \frac{2}{q\varepsilon N_d}(\psi + V) \qquad (1)$$

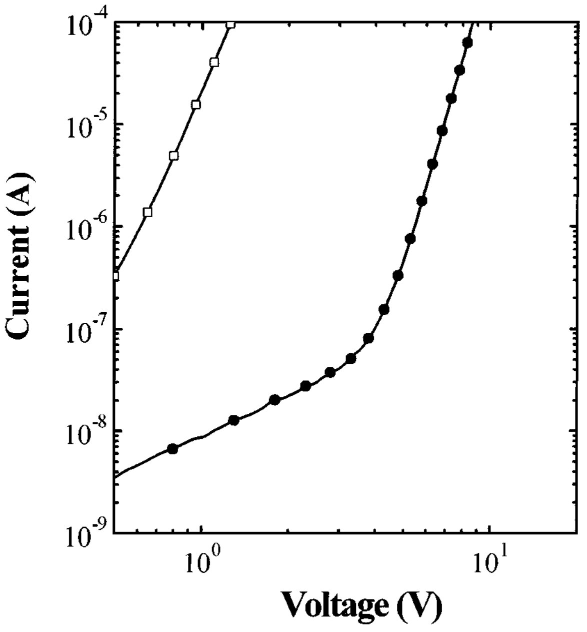

Figure 4 I-V characteristics of a single grain boundary of sintered specimen: □, without Na-diffusion; ●, with Na-diffusion.

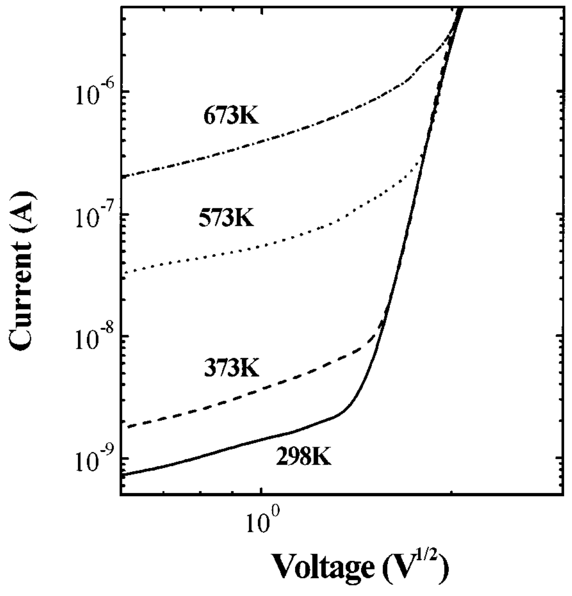

Figure 5 I-V characteristics of a single grain boundary of the Na-diffused specimen at various temperatures.

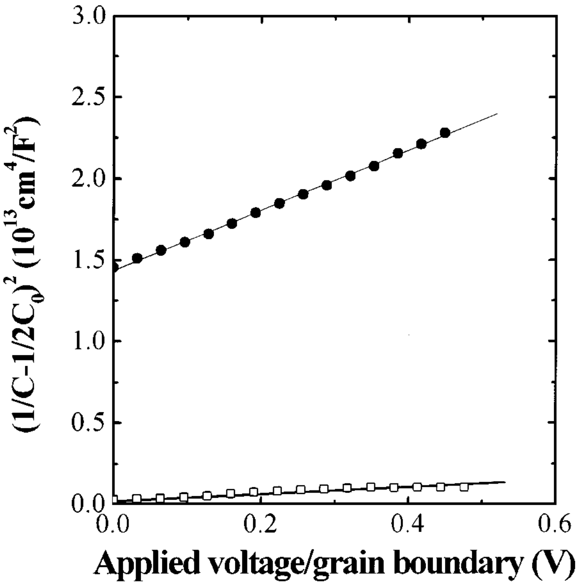

Figure 6 C-V measurement of the bulk specimen: □, without Na-diffusion; ●, with Na-diffusion.

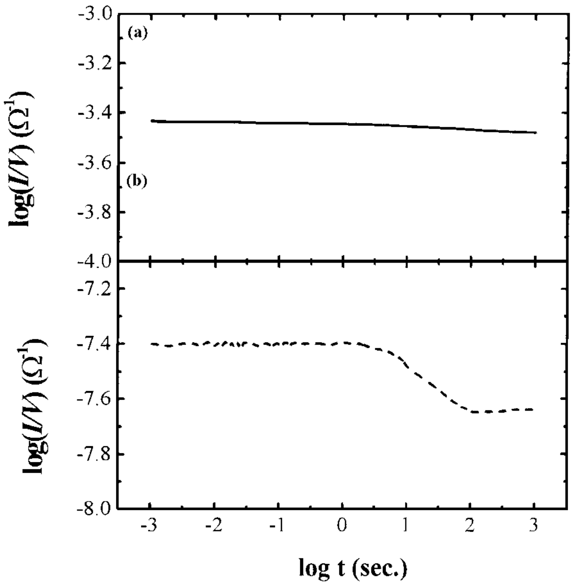

Figure 7 Current-Voltage ratio $|I/V|$ vs. time for a single grain boundary of the sintered specimen; (a) without Na-diffusion, (b) with Na-diffusion.

where C is the capacitance of a specimen at V, C_0 is the capacitance at $V = 0$, q is the electron charge, ε is the dielectric constant of SrTiO$_3$, V is the applied voltage per grain boundary. Fig. 6 shows the result of C-V measurement of $N1$ and $N2$ specimens. The potential barrier height ψ of $N1$ and $N2$ were obtained to be 0.82 and 0.14 eV, respectively.

3.4. Conductance measurement

In order to measure the conductance of bulk and grain boundaries at room temperature, dc voltage step technique with a micro-electrode method was also employed to observe the conductance of a single grain to grain junction at room temperature. This method allows the measurement of very high impedance but limited at very short times [20, 21]. Fig. 7 shows the results of conductances of specimens with and without the diffusion of Na against time. When Na was diffused in the grain boundaries of Nb-doped SrTiO$_3$, Maxwell-Wagner relaxation instead of Debye relaxation was found to be dominant. On the other hand, when annealed without the diffusion of Na, Debye relaxation was the dominant relaxation process. Maxwell-Wagner relaxation appears when there is a big difference in resistances between the grain and the grain boundary developed [22]. Therefore, it can be concluded that the diffusion of Na affected the electrical properties of grain boundaries.

3.5. Complex plane analysis

Complex plane analysis has already proven to be a useful means of characterizing the electrical nature of a

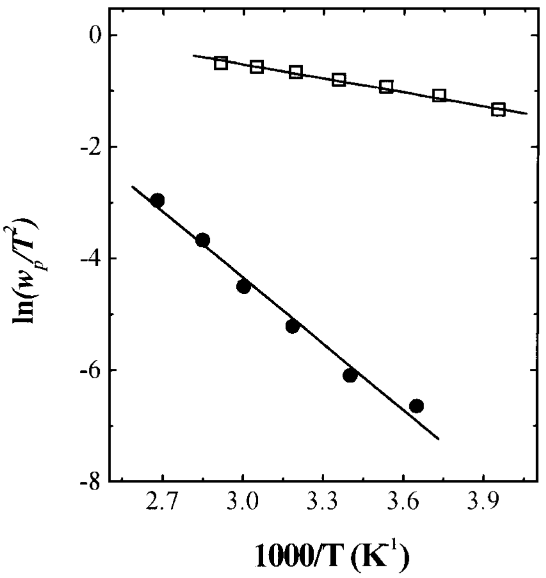

Figure 8 Arrhenious plots of $\ln(\omega_p/T^2)$ vs. $1000/T$ for a single grain boundary of the sintered specimen: □, without Na-diffusion; ●, with Na-diffusion.

number of heterogeneous materials [23, 24]. By applying small ac signal to the specimen, a relaxation occurs when the angular frequency of the ac signal becomes equal to the emission rate of electrons in a trapping state. Time dependency of ensuing charge transition is expressed via relation, described as Equation 2:

$$e_p = 1/\tau_p = \sigma_p v_{th} N_c \exp(-E_t/kT) \qquad (2)$$

where σ_p is the capture cross section of the trapping state, v_{th} is the free-electron thermal velocity, E_t is the activation energy and N_c is the conduction-band density of states. Thus, the slope of $\ln(\omega_p/T^2)$ versus $1000/T$, where ω_p is the peak frequency and T is the measured temperature, represents the activation energy of deep electronic defects. Fig. 8 provides the results of the deep electronic levels within the depletion regions formed at the grain boundaries of the specimen. The activation energies for $N1$ and $N2$ were found to be 0.10, 0.31 eV, respectively.

4. Discussion

$SrTiO_3$ was doped with 0.6 mol % Nb_2O_5 to carry semiconductive grains and Na was also diffused in grain boundary layers to improve varistor characteristics. When Nb_2O_5 is doped to $SrTiO_3$, the defect reaction occurs as described below [4]

$$Nb_2O_5 \rightarrow 2Nb^{\cdot}_{Ti} + 2e' + 4O^{x}_{o} + 1/2\,O_2$$

and $n = [Nb^{\cdot}_{Ti}]$, where n is the electronic concentration.

Since Na ions in the bulk of $SrTiO_3$ are more likely to substitute with Sr, it works as the source of grain boundary potential barrier with the diffusion of Na in grain boundaries. With Na replacing with Sr, the defect relation may be written as the following [4],

$$Na_2O \rightarrow 2Na'_{Sr} + 2h^{\cdot} + O^{x}_{o}$$

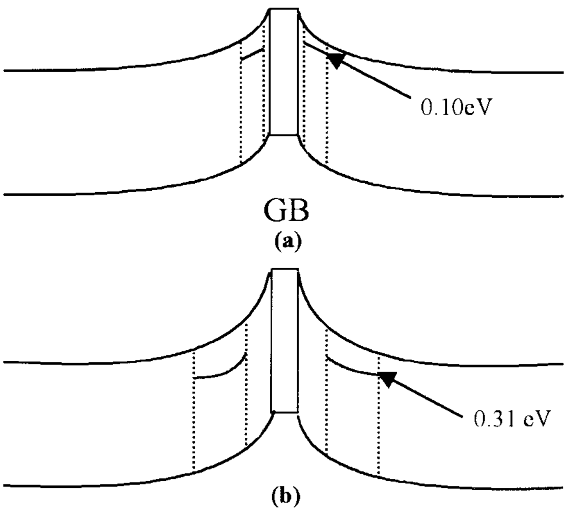

Figure 9 Qualitative energy schemes near grain boundary: (a) without Na-diffusion; (b) with Na-diffusion.

Sr substituted for Na becomes an acceptor that the negative charge is attained in the grain boundaries and this phenomenon would lead to a negatively charged grain boundary with a positively space-charge layer on either side [10]. Consequently, the potential barrier height is expected to increase with the diffusion of Na. In this study, it was confirmed that the potential barrier height of grain boundary is 0.82 eV from *C-V* measurement.

According to the data calculated from the complex plane analysis, it can be observed the deep electronic levels are changed with the diffusion of Na. If the substitution of Sr by Na affects the electronic states of grain boundaries, the electronic states of depletion region on either side of grain boundary were varied. When annealed in air without the diffusion of Na, 0.10 eV was obtained for the value of deep electronic level. The origin of this activation energy was postulated to be the value of electrons from oxygen vacancy state. After Na was diffused in grain boundaries, the measured value of activation energy was obtained to be 0.31 eV. Fig. 9 represents the energy scheme with and without the diffusion of Na. It shows that the electronic states of both grain boundaries and depletion regions were changed by the diffusion of Na in grains.

5. Conclusion

The influence of Na-diffusion on the electrical properties of $SrTiO_3$ was investigated in this study. When Na ions were diffused at 1000 °C, the segregation of Na ions was observed by SIMS analysis. It was also observed that the resistance of grain boundaries was significantly increased by the diffusion of Na. The non-linearity coefficient and the potential barrier height of Na-diffused specimen were found to be about 15 and 0.82 eV, whereas those of air-annealed specimen without the diffusion of Na was about 5, 0.14 eV respectively. This phenomenon, that the potential barrier height and the non-linearity coefficient of Na-diffused specimen were increased, might be explained by the substitution of Sr sites for Na ions. To verify this phenomenon, the change of electronic states in depletion region on either side of grain boundary was obtained. If the substitution of Sr by Na affects the electronic states of grain boundaries, the electronic states of depletion region on either side of grain boundary should be varied. From the complex plane analysis, it was obtained that the deep electronic levels near grain boundaries were changed from 0.10 to 0.31 eV.

Acknowledgements

The authors would like to express their thanks to Mr. Jin-O Cho at the McMaster University for his kindly support.

References

1. S. WAKU, *Rev. Electric. Commun. Lab.* **15** (1967) 689.
2. V. RAVIKAMURA, R. P. RODRIGUES and V. P. DRAVID, *J. Phys. D: Appl. Phys.* **29** (1996) 1799.
3. H. YAMADA and G. R. MILLER, *J. Solid State Chem.* **6** (1973) 169.
4. N. H. CHAN, R. K. SHARMA and D. M. SMYTH, *J. Electrochem. Soc.* **128** (1981) 1762.
5. M. FLEISHER, H. MEIXNER and C. TRAGUT, *J. Amer. Ceram. Soc.* **75** (1992) 1666.
6. R. M. GLAISTER and H. F. KAY, *Proc. Phys. Soc.* **76** (1960) 763.
7. K. MASUNO, T. MURAKAMI and S. WAKU, *Ferroelectrics* **3** (1972) 315.
8. I. BURN and S. NEIRMAN, *J. Mater. Sci.* **17** (1982) 3510.
9. M. FUJITOMO and W. D. KINGERY, *J. Amer. Ceram. Soc.* **68** (1985) 169.
10. M. FUJIMOTO, Y. M. CHANG, A. ROSHIKO and W. D. KINGERY, *ibid.* **68** (1985) C300.
11. N. YAMAOKA, *Amer. Ceram. Bull.* **65** (1986) 1149.
12. H. TOKANAMI and T. HATA, *ibid.* **74** (1995) 62.
13. D. KAINO, M. MASUYAMA and N. YAMAOKA, *J. E. E.* (1982) 103.
14. M. TOKANAMI and N. MAMADA, *ibid.* (1989) 50.
15. Q. ZOU and Z. MENG, *J. Amer. Ceram. Soc.* **78** (1995) 58.
16. R. WERNIKE, *Advance in Ceramics* **1** (1981) 272.
17. K. EDA, *J. Appl. Phys.* **49** (1978) 4453.
18. K. MUKAE, K. TSUDA and I. NAGASAWA, *ibid.* **50** (1979) 4475.
19. J. N. LIN, C. M. LIN, C. C. KAO and W. C. CHANG, *Mat. Sci. Eng.* **B20** (1993) 261.
20. M. VOLLMAN and R. WASER, *J. Amer. Ceram. Soc.* **77** (1994) 235.
21. R. WASER, *Solid State Ionics* **75** (1995) 89.
22. H. NEUMANN and G. ARLT, *Ferroelectrics* **69** (1986) 179.
23. M. A. ALIM, M. A. SEITZ and W. HIRTHE, *J. Appl. Phys.* **63** (1988) 2337.
24. S. N. BAI and T. Y. TSENG, *ibid.* **74** (1993) 695.

Received 25 August
and accepted 23 December 1998